

PowerPruning: Selecting Weights and Activations for Power-Efficient Neural Network Acceleration

Richard Petri¹, Grace Li Zhang², Yiran Chen³, Ulf Schlichtmann¹, Bing Li¹

¹Technical University of Munich, ²Technical University of Darmstadt, ³Duke University
Email: {richard.petri, ulf.schlichtmann, b.li}@tum.de, grace.zhang@tu-darmstadt.de, yiran.chen@duke.edu

Abstract

Deep neural networks (DNNs) have been successfully applied in various fields. A major challenge of deploying DNNs, especially on edge devices, is power consumption, due to the large number of multiply-and-accumulate (MAC) operations. To address this challenge, we propose PowerPruning, a novel method to reduce power consumption in digital neural network accelerators by selecting weights that lead to less power consumption in MAC operations. In addition, the timing characteristics of the selected weights together with all activation transitions are evaluated. The weights and activations that lead to small delays are further selected. Consequently, the maximum delay of the sensitized circuit paths in the MAC units is reduced even without modifying MAC units, which thus allows a flexible scaling of supply voltage to reduce power consumption further. Together with retraining, the proposed method can reduce power consumption of DNNs on hardware by up to 78.3% with only a slight accuracy loss.

1 Introduction

Deep neural networks (DNNs) have been successfully applied in various fields, e.g., image/speech recognition. In DNNs, a huge number of multiply-and-accumulate (MAC) operations with weights need to be executed, which correspondingly causes a high power consumption in hardware. This high power consumption poses challenges in applying DNNs on power-constrained computing scenarios, e.g., plant disease detection in agriculture [1] and medical diagnosis devices [2].

To overcome the challenge above, various methods on software and hardware levels have been explored. On the software level, pruning has been proposed to reduce the number of weights in DNNs and thus power consumption. For example, [3] proposes to prune weights with small absolute values to reduce the computation cost while maintaining inference accuracy. In addition, structure pruning [4] is further developed to facilitate the mapping of DNNs onto hardware. Besides pruning, quantization [5] is another major category of methods to reduce the computation cost of DNNs. With quantization, MAC units are implemented to process only integer instead of floating-point arithmetic, thus leading to a significant power reduction [6].

On the hardware level, various architectures have been proposed to explore how MAC units are organized and how data flow through the accelerators to reduce power consumption. The systolic array from Google [7, 8] adopts a weight-stationary data flow, where weights are stationary and activations and partial sums are moved across the array to maximize data reuse. Accordingly, the amount of memory access and thus power consumption can be reduced. In addition, the Eyeriss structure [9] uses a row-stationary data flow where the multiplication of rows of filters and activations is

computed in a MAC array to reduce data movement and thus power consumption.

The hardware architectures above have also been extended to reduce power consumption further. For example, a clock-gating scheme is proposed in [10] to disable the operations of unused MAC units to reduce dynamic power consumption. In [11], power-gating unused processing elements is proposed to reduce leakage power in idle hardware units. In addition, an earllystop technique in hardware has been proposed in [12] to skip unnecessary MAC operations, though a complex control logic is needed to implement this technique. Furthermore, GreenTPU in [13] scales the supply voltage of the computing logic down to near-threshold levels while keeping a high compute performance. But this method requires complex control logic to detect timing errors on-the-fly and to track activation sequences that cause timing errors. Similarly, Minerva [14] proposes a voltage scaling of memory units storing weights while exploiting the flexibility of neural networks to tolerate weight errors.

Different from the previous methods, most of which require special hardware architecture or control logic, we propose PowerPruning, a novel method exploiting the power and timing characteristics of weights and activations to reduce power consumption without modifying MAC units. PowerPruning is the first technique to evaluate the power and timing properties of each individual weight value and adjust neural networks accordingly. This technique is compatible with the previous methods for power reduction of executing neural networks and can be integrated with them seamlessly. The key contributions are summarized as follows:

- The power consumption of weight values is evaluated with respect to activations when the MAC operations are executed on hardware. Afterwards, weight values that lead to less power consumption in MAC operations are preferred for training neural networks to enhance the power efficiency.
- We consider the actual delays of the MAC operations in hardware with respect to weight values and activations. In training neural networks, the weight values and activations that sensitize paths with small delays are selected. Correspondingly, the circuit can run faster without modifying MAC units. We then scale the supply voltage to reduce the power consumption while maintaining the original computational performance.
- Neural networks are retrained by restricting weights and activations to the selected values while maximizing the inference accuracy. With the selected weights and activations, power consumption of DNNs can be reduced by up to 78.3% with only a slight accuracy loss.

The rest of the paper is structured as follows. Section 2 explains the motivation of this work. Section 3 elaborates the details of the

proposed technique. Experimental results are presented in Section 4 and conclusions are drawn in Section 5.

2 Motivation

In executing DNNs on hardware platforms, the huge number of MAC operations may consume much power. Existing methods often introduce hardware modifications, which may incur extra hardware cost or make the design specific for individual neural networks. On the contrary, we address this power consumption issue by examining the power and timing properties of the weight values and activations.

A MAC unit calculates the multiplication of a weight and an activation and adds the result to a partial sum, as illustrated in Figure 1. Assume the weight of a neural network is quantized to n bits. Correspondingly, there are 2^n possible weight values. These weight values are one of the inputs to the digital logic implementing the MAC operations. Since different weight values cause different signal switching activities inside the MAC units, they also exhibit different average power consumption with respect to the activation transitions and partial sum transitions. For example, the weight values 2^n , $n = 0, 1, \dots, n - 2$, lead to less power consumption, because the multiplication with these weight values are actually shift operations and can thus activate fewer signal propagations in the circuit.

To demonstrate the different power consumption of weight values, we evaluated the average power consumption of different weight values in a MAC unit of a 64×64 systolic array. We simulated the execution of LeNet-5 processing 100 pictures randomly selected from the CIFAR-10 dataset. During simulation, we collected statistics of the switching activities of various signals inside the systolic array. Based on this data we estimated the average power consumption of each weight value using Power Compiler from Synopsys.

Figure 2 illustrates the average power consumption of the weight values obtained by the simulation described above. According to this figure, different weight values can lead to substantially different average power consumption. For example, the quantized weight value -105 has a large average power consumption $1,029 \mu\text{W}$, while the quantized weight value -2 has only $539 \mu\text{W}$. *According to this observation, by restricting neural networks to prefer the weight values with small average power consumption, the overall power consumption of executing neural networks can be lowered.*

Besides different power characteristics, different weights also exhibit different timing profiles in a MAC unit. Inside a MAC unit shown in Figure 1, there are many combinational paths, which have different delays and are triggered by specific input data, i.e., weight, activation, and partial sum. If the weight is fixed to a given value, some combinational paths in the MAC unit cannot be sensitized. Accordingly, the delay of the MAC unit may differ with respect to different weight values. To demonstrate this difference, we conducted timing analysis of the MAC unit with fixed weight values and all activation transitions using Modelsim.

Figure 3 illustrates the delay profiles of two quantized weight values -105 and 64, where the x-axis shows the delay and the y-axis shows the frequency of this delay appearing with respect to all possible activation transitions. Figure 3 confirms that different weight values lead to different delays. In addition, it shows that the delays can be reduced further if some activations can be pruned from the neural network, e.g., the activation transitions triggering delays on the far right end of the x-axis. *Since the clock period of a circuit is determined by the maximum delay of all the combinational*

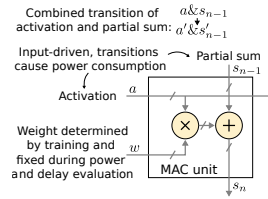


Figure 1: Power and delay characterization of MAC unit.

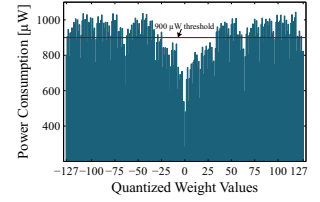


Figure 2: Average power consumption of quantized weight values.

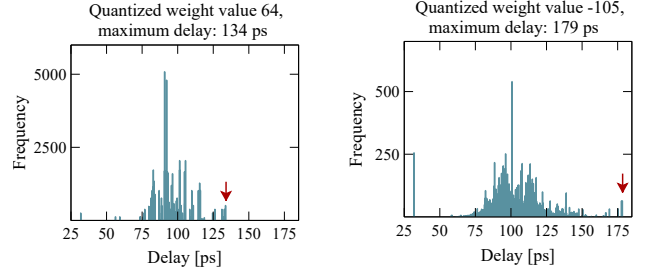


Figure 3: Delay profiles of a MAC unit for two quantized weight values. The arrows point to the maximum delay of a given weight value with respect to all the activation transitions.

paths, the clock frequency of the MAC unit and thus the computational performance can be increased by pruning weights and activations according to their timing profiles. Alternatively, the supply voltage can be lowered to reduce power consumption further, while maintaining the original clock frequency.

3 Weight and Activation Selection for Power-Efficient Neural Network Acceleration

In this section, we introduce the proposed PowerPruning method to reduce power consumption in digital neural network accelerators. The weight selection according to the average power consumption is first explained in Section 3.1. Afterwards, the selection of weights and activations with respect to their timing characteristics is explained in Section 3.2. The retraining of neural networks by restricting weights and activations to the selected values to reduce power consumption is described in Section 3.3.

3.1 Weight selection according to power consumption

As shown in Figure 2, different weights in a MAC unit lead to different average power consumption. To take advantage of this characteristic to reduce power consumption of DNN accelerators, the average power consumption of all the 8-bit integer weight values in a MAC unit should be evaluated. To do this, the input of the MAC unit corresponding to the weight is fixed to a given value, as shown in Figure 1. The various combinations of activation transitions and partial sum transitions are fed into the other inputs of the MAC unit to obtain the switching activities of the MAC unit. Based on these switching activities the power consumption for the fixed weight value can be evaluated using Power Compiler from Synopsys.

Two challenges in evaluating the average power consumption of a weight should be addressed. First, the number of combined transitions of activations and partial sums is huge, e.g., $2^{(8+22) \times 2} = 2^{60} \approx 10^{18}$, when the activations and the partial sums are quantized to 8 and 22 bits, respectively, for a 64×64 systolic array. $\times 2$ is due to the fact that the power consumption is caused by the transitions

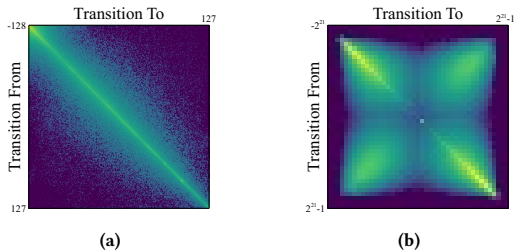


Figure 4: Transition distributions of activations and partial sums of a MAC unit. (a) Activation transition distribution. (b) Partial sum transition distribution.

from a combination of activation and partial sum to another combination, instead of the static values of the activation and partial sum. Accordingly, simulating all these transitions to identify the power consumption is very time-consuming. Second, just sampling all possible combined transitions of activations and partial sums does not reflect the probabilities of such transitions when executing neural networks in a systolic array. For example, a combined transition may appear more frequently than other transitions, so that it should contribute more to the result of power evaluation than others.

To deal with these challenges, we first identify the transition distributions for activations and partial sums with real data executing on the systolic array, described as follows. In addition, we partition the value range of the partial sum into a small number of bins to reduce the partial sum transition space and then evaluate the transition probability from one bin to another bin.

3.1.1 Evaluation of activation transition distribution For the 8-bit activation as an input to a MAC unit, the total number of possible transitions is $2^{8 \times 2} = 2^{16}$. To obtain the activation transition distribution, we simulate the activities of a systolic array and count the frequency of each individual transition. For example, for LeNet-5 on CIFAR10, we randomly select 100 pictures and execute the neural network on the systolic array. In total we counted approximately 10^{17} activation transitions. Since this number is larger than the number of possible transitions 2^{16} , the result will well exhibit the distribution of the activation transitions.

Figure 4(a) shows the resulting activation transition distribution, where darker colors represent a lower probability and brighter colors a higher probability. In this figure, the bright diagonal line clearly indicates that most transitions appear between activations with similar values, while activation transitions from very high to very low values and vice versa are very unlikely to happen.

3.1.2 Evaluation of partial sum transition distribution and transition space reduction A partial sum has 22 bits in a systolic array with the size of 64×64 , which results in $2^{22 \times 2} = 2^{44} \approx 1.8 \times 10^{13}$ possible transitions. If we would simulate 100 pictures on the systolic array, we can obtain approximately 2.2×10^8 partial sum transitions, which is much smaller than the number of possible transitions and cannot produce a trustworthy distribution. Increasing the number of pictures in simulation is not a viable solution due to runtime. To solve this problem, we partition the value range of the partial sum into a small number of bins. Accordingly, instead of evaluating the transition probability of individual partial sum values, we evaluate the transition probability from one bin to another bin.

To partition all partial sums into a small number of bins, we should guarantee that in each bin the switching activities of partial sums should be kept as similar as possible. We partition the partial sums

Table 1: Bounds for selected bins for partial sum partition.

Bin index	Lower bound	Upper Bound
0	10000000000000000000000000000000	1011111111111111111111111111111111
8	11111111110000000000000000000000	1111111110101111111111111111111111
9	11111111110000000000000000000000	1111111111011111111111111111111111
34	00000000010000000000000000000000	0000000001111111111111111111111111
35	00000000100000000000000000000000	0000000011111111111111111111111111
42	01000000000000000000000000000000	0111111111111111111111111111111111

by keeping the number of consecutive most significant bits with the same value as large as possible. Table 1 lists the lower and upper bounds of some selected bins. All values which are in the same bin have the same number of consecutive most significant bits with the same value. In total, we end up with 43 bins. This partition of the partial sums allows us to capture how many most significant bits either stay constant if during a transition the sign does not change, or how many most significant bits change if the sign changes during a transition. This binning approach is only a heuristic solution and future work is needed to capture the bit-switching characteristics of the partial sums more accurately.

After the partition of partial sums into bins, we simulated 100 pictures and assigned the real transitions into these bins. Afterwards, the probabilities of the transitions between bins can be identified, similar to the evaluation of the activation transition distribution in Section 3.1.1. Figure 4(b) shows the partial sum transition distribution of the bins. It can be observed that the full value range of the partial sums are rarely used. The bright diagonal line from the upper left to the lower right corner indicates that there are many transitions between partial sums with similar values. However, there is also a slightly weaker diagonal line from the upper right to the lower left corner, showing that a portion of partial sums changes their signs during transitions and causes relatively large switching activities.

3.1.3 Weight selection With the distributions identified above, we sample 10,000 transitions of both activations and partial sums according to their probabilities. The combined transitions are used to simulate the activities of the MAC unit with the weight input fixed to specific values. The resulting switching activities are then used to calculate the average power consumption of the MAC unit for this weight. This simulation is repeated for each individual weight value and the result is shown in Figure 2, where the power consumption of each weight varies greatly. In this result, there is also a trend that weights close to zero have especially low power consumption, with weight zero having by far the lowest.

Based on the result of power analysis we first conduct conventional pruning to maximize the number of weights with zero value to reduce power consumption. Afterwards, we select weight values that lead to small power consumption by setting a power threshold, e.g., $900 \mu\text{W}$ in Figure 2. By setting the threshold lower, we can achieve potentially more power savings by excluding more high-power weight values. However, the accuracy of the DNN may degrade. Therefore, a tradeoff between power saving and inference accuracy should be made.

3.2 Weight and activation selection according to timing profiles

According to Figure 3, weight values exhibit different timing characteristics. Even for the same weight, different activation transitions lead to different delays. To identify weight values and activations with small delays, the timing of each weight value with respect to activation transitions and partial sum transitions in the MAC unit

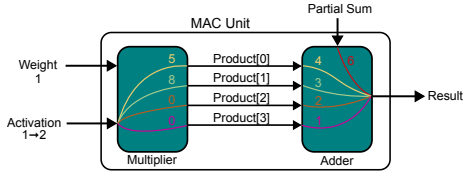


Figure 5: Concept of timing analysis of the MAC unit.

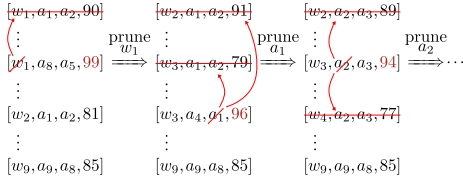


Figure 6: Concept of weight and activation selection for delay reduction.

should be analyzed. Two types of timing analysis methods, dynamic timing analysis and static timing analysis, are available for this task. The former is conducted by applying input transitions into a circuit and evaluating the delays of correspondingly triggered paths, while the latter evaluates the delay statically without considering the corresponding triggered paths. The latter is conservative since the delays of some paths that are not activated are also included and the clock frequency of the circuit may be unnecessarily lowered.

To evaluate the timing profile of a weight value, an intuitive idea is to fix the weight input into the MAC unit and then apply dynamic timing analysis with all the transition patterns of activations and partial sums to simulate the unit. The challenge of this method is that the number of combined transitions of activations and partial sums is huge, as described in Section 3.1. Simulating the delay of the MAC unit with respect to all these combinations is thus time-consuming.

To reduce the runtime of timing analysis, we separate the timing analysis of the multiplier and adder in the MAC unit. Specifically, we apply static timing analysis on the adder to avoid the consideration of input transitions, because the number of inputs to the adder is very large. On the other hand, the multiplier is evaluated using accurate dynamic timing analysis, since the delay of the multiplier usually dominates the delay of the MAC unit and this delay can be lowered by filtering out some weight values and activation values.

To conduct dynamic timing analysis of the multiplier for a weight value, we simulate the multiplier by fixing the weight input and enumerating the $2^{8 \times 2}$ possible transitions of the activations. Static timing analysis of the adder is conducted by the built-in timing analyzer in Design Compiler from Synopsys. To incorporate the relation between the timing paths in the multiplier and the adder, we evaluate the largest delay starting from each individual bit of the product to the output of the adder. Afterwards, the largest delay of the MAC unit with respect to the given weight value is calculated by adding the delays from the input activation to the output bits of the multiplier and the delays from the corresponding product bits to the output of the adder.

Figure 5 illustrates the concept of timing analysis of the MAC unit, where the quantized weight 1, the activation transition from quantized 1 to quantized 2, and four product bits at the output of the multiplier are used as example. With the dynamic timing analysis applied on the multiplier, the delays from the input activation to Product[0] and Product[1] are 5 and 8, respectively. The delays to the other two product bits can be 0 if the combinational paths to them

are not activated by the activation transition. With static timing analysis applied on the adder, the delays from the output bits of the multiplier to the output of the adder are 4, 3, 2, 1, respectively. Assume the delay from the partial sum to the output of the adder is 6 returned by static timing analysis. The largest delay of the MAC unit is thus $\max\{5 + 4, 8 + 3, 6\} = 11$.

The timing analysis method described above is applied for each weight individually. After that, all the delays of weights with respect to activation transitions can be obtained. To select weights and activations with small delays, we first set a delay threshold and iteratively remove weights or activations that lead to delays larger than the given threshold. The iterations end until all the delays of the remaining weights and activations are smaller than the given delay threshold. Figure 6 illustrates an example with the delay threshold set to 90. In the first step, we find the largest delay 99. Since 99 is larger than the specified threshold, we have to remove either w_1 , a_5 or a_8 to exclude the corresponding combination. Since the removal of either w_1 , a_5 or a_8 also affects other combinations in Figure 6, it is difficult to find the optimal sequence to remove the weights and activations. Accordingly, we randomly remove any of them and then remove the other combinations containing the removed weight or activation in Figure 6. For example, removing w_1 also leads to the removal of the first combination in Figure 6. To avoid local optimum, we execute this process several times and choose which weight or activation to remove in each step randomly. The removal process ends when the maximum delay of all the combinations is lower than the given threshold 90. The result is a set of weights and activations that satisfy the delay requirements. While pruned weight values can be avoided during training of neural networks, the filtering of activations needs to be integrated into the activation function after each layer.

3.3 Neural network training for power reduction

To reduce power consumption of DNNs on hardware, we first apply conventional pruning to remove weights whose absolute values are close to zero. Afterwards, we select weights that lead to small power consumption by setting a power threshold. The initial power threshold is $900 \mu W$ and it is iteratively reduced by $50 \mu W$ to select weights. In each iteration, the neural networks are retrained with the selected weights to verify the inference accuracy. During retraining, we force the weights to take the restricted values in the forward propagation. In the backward propagation, the straight through estimator [15] is adopted to skip the restriction operation. The iterations end when the inference accuracy starts to drop noticeably.

After the power threshold is determined, we then select weight values and activations that lead to small delays by setting a delay threshold. The initial delay threshold is $170 ps$ and the delay threshold is iteratively reduced by $10 ps$ to select weight values and activations. In each iteration, the neural networks are retrained and verified. When the inference accuracy drops by around 5% of the original inference accuracy of the neural networks, the best training result is returned.

When executing the neural networks, if the original clock frequency should be maintained, we can lower the supply voltage to reduce power reduction. We use the results in [16] to determine the relation between supply voltage and the delay of the circuit. The scaling of dynamic power consumption and leakage is conducted according to [17].

Table 2: Experimental results of proposed method.

Network-Dataset	Accuracy		Total Power Consumption [mW]						#Selected		Max Delay	Voltage Scaling		
			Standard HW		Optimized HW		Red.	Factor				V_SHW	V_OHW	
	Orig.	Prop.	Orig.	Prop.	Red.	Orig.			Prop.	Red.	Wei.			Act.
LeNet-5-CIFAR-10	80.6%	78.5%	375.5	149.6	60.2%	360.7	78.3	78.3%	35	210	40 ps	0.71/0.8	10.1%	5.4%
ResNet-20-CIFAR-10	91.9%	89.6%	718.9	361.0	49.8%	663.9	288.3	56.6%	35	210	40 ps	0.71/0.8	13.2%	11.5%
ResNet-50-CIFAR-100	79.9%	78.5%	708.7	293.8	58.5%	701.8	157.1	77.6%	41	223	30 ps	0.73/0.8	8.1%	4.2%
EfficientNet-B0-Lite-ImageNet	73.8%	69.7%	21.2	19.3	9.0%	2.4	1.9	20.8%	50	236	20 ps	0.75/0.8	6.4%	6.5%

4 Experimental Results

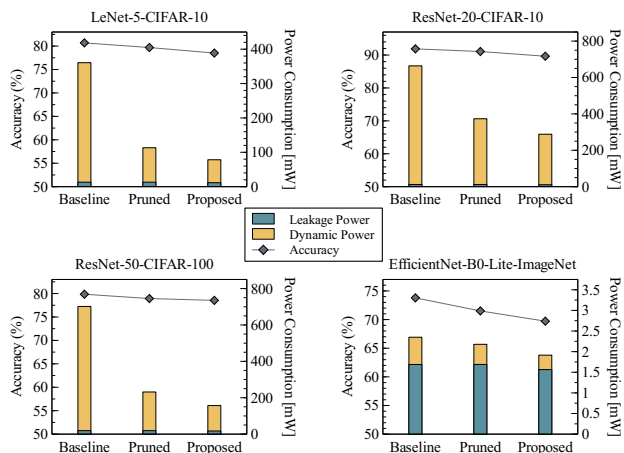
To verify the proposed method, we tested four different neural network and dataset combinations, as shown in the first column of Table 2. The weights and activations were quantized to eight bits. The neural networks were trained using Tensorflow while considering quantization [5]. In Tensorflow, the number of 8-bit weights is 255 instead of 256 to maintain the weight distribution symmetrical while the number of 8-bit activations is 256. After training, small weights were pruned to compress the neural network. We then applied the proposed method to reduce the power consumption. For LeNet-5, ResNet-20 and ResNet-50, Nvidia Quadro RTX 6000 GPU 24 GB was used for training, and for EfficientNet-B0-Lite Nvidia A100 80 GB GPU was used. The number of times to execute the selection of weight and activation with small delays in Section 3.2 is set to 20 in the experiments.

To demonstrate the effectiveness of the proposed method on different types of accelerators, two different hardware implementations of systolic array were evaluated. In the optimized hardware architecture (Optimized HW), clock gating of a MAC unit in case of a zero weight to reduce dynamic power consumption and power gating of whole unutilized columns in the systolic array to reduce both the dynamic and static power consumption are applied. In the standard architecture (Standard HW), none of these power-saving features were applied.

The power consumption during inference was estimated with Power Compiler by simulating the systolic array executing the neural networks using Modelsim. The simulation was conducted using a netlist description of the systolic array synthesized with the NanGate 15 nm cell libraries [18] and the clock frequency around 5 GHz. Since cycle-accurate simulations are extremely time-consuming, for ResNet-20, ResNet-50 and EfficientNet-B0-Lite only the convolutional layers with the largest number of MAC operations were simulated and compared.

Table 2 summarizes the experimental results of the proposed method. The original accuracy and the accuracy with our method are shown in the second and third columns. According to these two columns, the accuracy degradation is relatively small, except for EfficientNet-B0-Lite with a drop of 4%. With a slight accuracy loss, a significant reduction in power consumption up to 78.3% can be achieved, as shown in the sixth and ninth columns, demonstrating the effectiveness of the proposed method in enhancing power efficiency of digital accelerators for neural networks. This is especially useful for edge devices where power consumption is a major issue.

When executing the neural networks on Standard HW, the total power including dynamic and leakage power was reduced by up to 60.2% (sixth column). On Optimized HW, the power saving was even greater with a power reduction up to 78.3% (ninth column). The relatively smaller power reduction on Standard HW was caused


Figure 7: Comparison with conventional pruning, evaluated on Optimized HW.

by the leakage power consumption from the MAC units that were not gated even when they are not used. In all the cases, the power consumption of EfficientNet-B0-Lite was not reduced significantly. This was due to their depth-wise 2D convolutions, which had a very low utilization rate of the systolic array and thus high execution time, so that the dynamic power consumption was much lower than the leakage power.

To reduce the maximum delay of a MAC unit, which was 180 ps after synthesis, we only selected a subset of weight values and activations that lead to small delays of the MAC operations. The number of selected weight values and selected activation values are shown in the tenth column (Wei.) and the eleventh column (Act.). According to the tenth column, the number of selected weight values is reduced significantly, e.g., from 255 to 35 in LeNet5 and ResNet-20. On the contrary, most activation values still remain to maintain a good inference accuracy. The delay reduction due to the weight and activation selection is shown in the twelfth column (Max Delay Red.). In identifying delay reduction, our search granularity was 10 ps. This can be lowered if necessary, but at the expense of more runtime.

To reduce power consumption further, the supply voltage is lowered by the ratio shown in thirteenth column (Voltage Scaling Factor). For example, for LeNet-5-CIFAR-10, the supply voltage was reduced from 0.8 V to 0.71 V while still maintaining the original clock frequency. The relation between supply voltage scaling and circuit delay was evaluated according to the simulation results in [16]. The last two columns show the percentage of power reduction contributed by voltage scaling. For Standard HW (column V_SHW) and Optimized HW (column V_OHW), voltage scaling can reduce power consumption by up to 13.2% and 11.5%, respectively.

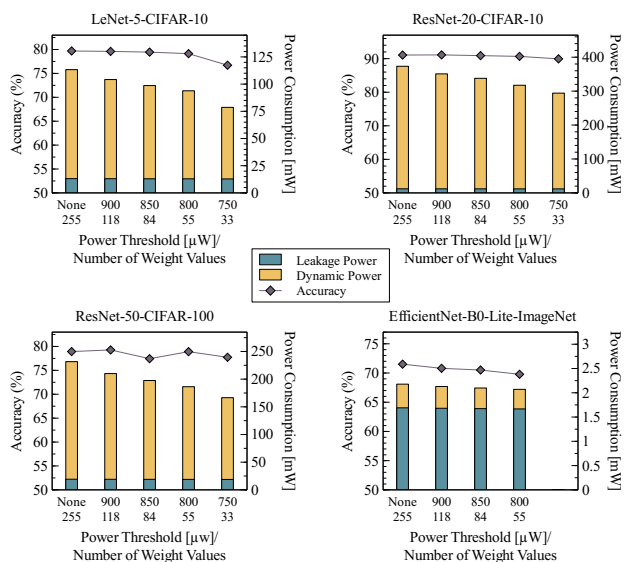


Figure 8: Tradeoff between accuracy and the number of selected weight values, evaluated on Optimized HW.

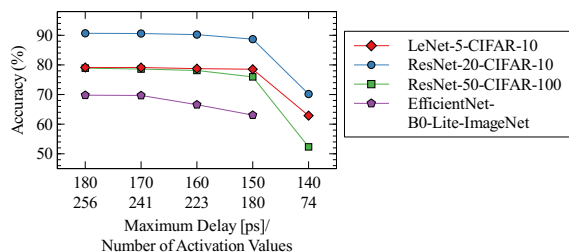


Figure 9: Tradeoff between accuracy and the number of selected activation values.

To demonstrate the advantage of the proposed method over conventional pruning, we show the comparison of the power consumption and the inference accuracy of conventional pruning and the proposed method in Figure 7. According to this comparison, the proposed method can significantly reduce the power consumption of a pruned neural network further with only a slight accuracy loss. The proposed method achieves better power savings when the dynamic power consumption dominates the overall power consumption, e.g., the first three comparisons in Figure 7, because it focuses on reducing the signal switching activities in the circuits by selecting weights.

To demonstrate the tradeoff between the number of selected weight values and the inference accuracy, we used different thresholds to select weight values according to their power consumption and evaluated the accuracy by restricting the neural networks to these weight values. Figure 8 illustrates the results. As expected, a lower power threshold leads to a lower inference accuracy. However, there is still a good potential for power reduction before significant accuracy degradation appears. For example, for ResNet-50-CIFAR-100 the power threshold can be lowered down to 800 μ W, which corresponds to 55 weight values, leading to total power savings of 19.6% with only a negligible accuracy loss. Note that the drop at 850 μ W for ResNet-50-CIFAR-100 is due to the stochastic nature of

the training process. For EfficientNet-B0-Lite the power reduction is relatively small due to the large contribution of leakage power.

Figure 9 shows the tradeoff between accuracy and the number of activation values. The results are obtained by restricting neural networks with different number of activation values based on a weight selection threshold 800 μ W. The different numbers of activation values reflect different maximum delays on the MAC unit. In this figure, the left most point corresponds to the full activation space with 256 activation values. As the number of activation values and thus the maximum delay decreases, the inference accuracy is first well-maintained and then drops. Before the turning point, there is optimization potential we took advantage of to enhance computational performance or reduce power consumption by voltage scaling.

5 Conclusion

In this paper, we have proposed PowerPruning, a novel method to reduce power consumption in digital neural network accelerators by selecting weights that lead to less power consumption in MAC operations. The timing characteristics of the selected weights together with activation transitions are also evaluated. We then selected weights and activations that lead to small delays, so that either the clock frequency of the MAC units can be improved or voltage scaling can be applied to reduce power consumption further. Together with retraining, the proposed method can reduce power consumption of DNNs on hardware by up to 78.3% with only a slight accuracy loss. The proposed method does not modify MAC units and can be combined seamlessly with existing hardware architectures for power-efficient neural network acceleration.

References

- [1] W.-L. Chen *et al.*, "RiceTalk: Rice blast detection using internet of things and artificial intelligence technologies," *IEEE Internet of Things Journal*, vol. 7, no. 2, 2020.
- [2] S. Hassantabar *et al.*, "MHDeep: Mental health disorder detection system based on wearable sensors and artificial neural networks," *ACM Trans. Embed. Comput. Syst.*, 2022.
- [3] S. Han *et al.*, "Deep compression: Compressing deep neural network with pruning, trained quantization and Huffman coding," in *International Conference on Learning Representations (ICLR)*, 2016.
- [4] W. Wen *et al.*, "Learning structured sparsity in deep neural networks," in *International Conference on Neural Information Processing Systems (NIPS)*, 2016.
- [5] B. Jacob *et al.*, "Quantization and training of neural networks for efficient integer-arithmetic-only inference," in *IEEE/CVF Conference on Computer Vision and Pattern Recognition (CVPR)*, 2018.
- [6] A. Gholami *et al.*, "A survey of quantization methods for efficient neural network inference," *CoRR*, 2021.
- [7] N. P. Jouppi *et al.*, "In-datacenter performance analysis of a tensor processing unit," in *International Symposium on Computer Architecture (ISCA)*, 2017.
- [8] "Edge TPU," <https://cloud.google.com/edge-tpu>.
- [9] Y.-H. Chen *et al.*, "Eyeriss: An energy-efficient reconfigurable accelerator for deep convolutional neural networks," *IEEE Journal of Solid-State Circuits (ISSCC)*, vol. 52, no. 1, 2017.
- [10] N. D. Gundi *et al.*, "EFFORT: Enhancing energy efficiency and error resilience of a near-threshold tensor processing unit," in *Asia and South Pacific Design Automation Conference (ASP-DAC)*, 2020.
- [11] P. Pandey *et al.*, "UPTPU: Improving energy efficiency of a tensor processing unit through underutilization based power-gating," in *ACM/IEEE Design Automation Conference (DAC)*, 2021.
- [12] V. Akhlaghi *et al.*, "SnaPEA: Predictive early activation for reducing computation in deep convolutional neural networks," *International Symposium on Computer Architecture (ISCA)*, 2018.
- [13] P. Pandey *et al.*, "GreenTPU: Improving timing error resilience of a near-threshold tensor processing unit," in *ACM/IEEE Design Automation Conference (DAC)*, 2019.
- [14] B. Reagen *et al.*, "Minerva: Enabling low-power, highly-accurate deep neural network accelerators," in *ACM/IEEE International Symposium on Computer Architecture (ISCA)*, 2016.
- [15] Y. Bengio *et al.*, "Estimating or propagating gradients through stochastic neurons for conditional computation," *ArXiv*, 2013.
- [16] W. Lee *et al.*, "Dynamic thermal management for FinFET-based circuits exploiting the temperature effect inversion phenomenon," in *IEEE/ACM International Symposium on Low Power Electronics and Design (ISLPED)*, 2014.
- [17] N. Pinckney *et al.*, "Impact of FinFET on near-threshold voltage scalability," *IEEE Design & Test*, vol. 34, no. 2, 2017.
- [18] "15nm Open-Cell library and 45nm freePDK," <https://si2.org/open-cell-library/>.